INVESTIGATION OF A MONOLITHIC, INTEGRATED-CIRCUIT, DIFFERENTIAL AMPLIFIER AS A MIXING DEVICE

by

Robert Conrad McFarland

UNITED STATES
NAVAL POSTGRADUATE SCHOOL

THESIS

INVESTIGATION OF A MONOLITHIC, INTEGRATED-CIRCUIT,

DIFFERENTIAL AMPLIFIER AS A MIXING DEVICE

by

Robert Conrad McFarland

September, 1968

INVESTIGATION OF A MONOLITHIC, INTEGRATED-CIRCUIT, DIFFERENTIAL AMPLIFIER AS A MIXING DEVICE

by

Robert Conrad McFarland
Lieutenant, U.S. Coast Guard
B.S., Coast Guard Academy, 1961

[redacted]

Submitted in partial fulfillment of the
requirement for the degree of

MASTER OF SCIENCE IN ELECTRICAL ENGINEERING

from the

NAVAL POSTGRADUATE SCHOOL
September, 1968

ABSTRACT

The balanced, differential-amplifier configuration finds wide applicability in its monolithic integrated form. This paper investigates the use of the MIC differential amplifier as a mixer. The device chosen for this investigation permits signal injection both in the differentially driven pair and in the constant-current sink which biases the differential pair. Device characteristics pertinent to the mixing process are generated and discussed. On the basis of the experimentally derived characteristics, several different frequency conversion methods are employed and compared on the basis of conversion gain and distortion and intermodulation effects.

TABLE OF CONTENTS

LIST OF ILLUSTRATIONS

1. Introduction

The balanced differential amplifier finds wide use in linear integrated-circuit applications. This paper investigates the mixing characteristics of the CA-3005[1], which was chosen as representative of a variety of such basic circuits from several manufacturers. Initially, the device characteristics are developed by measurement and these are discussed. This is followed by a description of the frequency-conversion process as it relates to the experimentally derived characteristics.

Three different conversion techniques are studied in detail. In the first method, signal and local-oscillator voltages are impressed on the differential input. In the second, the signal voltage is injected at the differential input, while the local oscillator voltage is placed at the base of the constant-current sink. Thus, in this latter method, the oscillator injection controls the total emitter-collector current in the differential pair. In the third method, the signal voltage controls the constant-current sink, while the local oscillator voltage is injected into the differential pair. In each of the three basic methods, conversion gain is measured as a function of local-oscillator injection level. The effect of DC-offset in the differential pair on the conversion gain is also investigated.

Since it is primarily the symmetry of the transconductance characteristics that distinguishes this device from other small-signal mixing devices, this property is used to advantage in two applications. In the first, the configuration is connected to provide carrier cancellation at the output. This permits the use

of larger local-oscillator injection voltage without saturating subsequent amplifier stages. The second takes advantage of the even-order function describing the transconductance curve. Properly biased, the output is strong in even-order harmonics while the fundamental and odd harmonics are very low. This would permit the use of a local oscillator designed to operate at half the frequency ordinarilly required to superimpose the signal on a carrier of designated frequency.

The appendices include suggested laboratory exercises which illustrate the important features, and describe the experimental procedures used in obtaining the data for this investigation.

2. Description of the Device

The balanced differential amplifier is a basic circuit configuration used for a broad line of all-monolithic, silicon integrated circuits (MIC) and is designed for a wide variety of linear applications at frequencies from dc into the vhf region. The circuit, illustrated in figure 2.1, finds wide use in the monolithic form because of its great versatility.

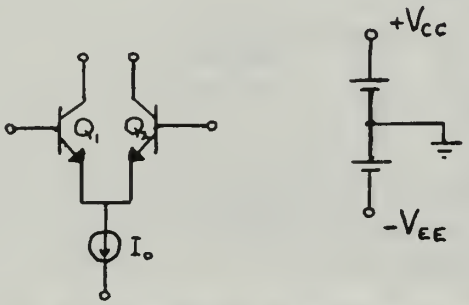

Figure 2.1: Basic Differential Amplifier

This circuit permits single or double-ended inputs and outputs, linear amplification from dc through the vhf region, good isolation between output and input, and simplifies the use of feedback when required. Because of its monolithic form, electrical symmetry of Q_1 and Q_2 can be attained very closely, since they are simultaneously and identically processed in adjacent locations on a common chip. Also, the configuration and the biasing arrangement eliminates the need for by-pass capacitors.

The particular MIC device chosen for this experiment was the RCA CA-3005 Integrated-Circuit RF Amplifier. This circuit is readily available as an off- the -shelf item, is inexpensive and provides access leads at every node. An analysis of this circuit, leading to

the transfer curves and hence to the transconductance curves for this device, is necessary preliminary to the investigation of its mixing characteristics[2]. The CA-3005 is shown schematically in figure 2.2.

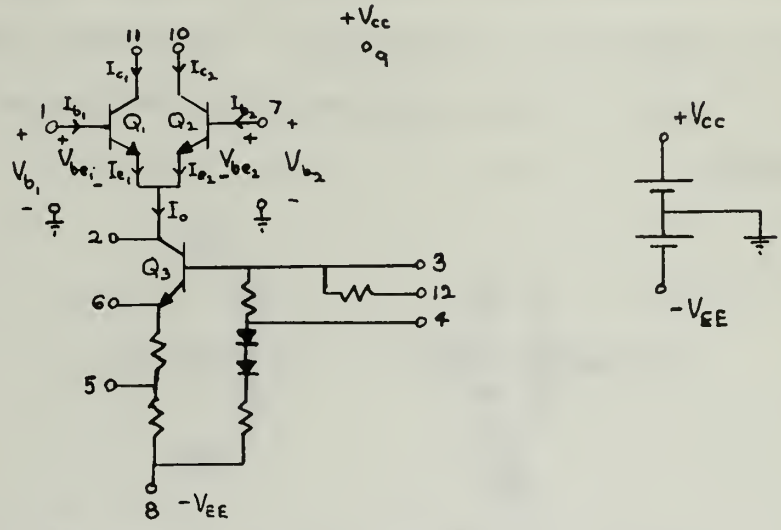

Figure 2.2: Schematic Diagram of CA-3005

Initially we will ignore Q_3 and substitute a current generator, I_o in its place. The following basic relations hold.

Basic Relations

(1) $I_{e_1} + I_{e_2} = I_o$

(2) $I_c = \alpha I_e$

(3) $I_b = (1 - \alpha) I_e$

(4) $I_e = I_s (e^{\frac{q V_{be}}{kT}} - 1) \approx I_s (e^{\frac{q V_{be}}{kT}})$

(5) $V_{be_1} - V_{be_2} = V_{b_1} - V_{b_2}$

We assume that Q_1 and Q_2 are electrically identical. Then,

$$\alpha_1 = \alpha_2 = \alpha, \; I_{s_1} = I_{s_2} = I_s, \; T_1 = T_2 = T$$

By substituting (4) into (1), we can solve for I_s in terms of I_o and V_{be}. Using this result in (4) we have I_e in terms of I_o and V_{be}. Finally, using (2) we have I_c in terms of I_o and V_{be}. The collector current transfer equations are:

$$(6) \quad I_{c_1} = \frac{\alpha I_o}{1 + e^{\frac{(V_{b_2} - V_{b_1})q}{kT}}} \qquad I_{c_2} = \frac{\alpha I_o}{1 + e^{\frac{-(V_{b_2} - V_{b_1})q}{kT}}}$$

A plot of I_{c_1}, I_{c_2} versus differential input voltage is shown in figure 2.3 for several values of I_o.

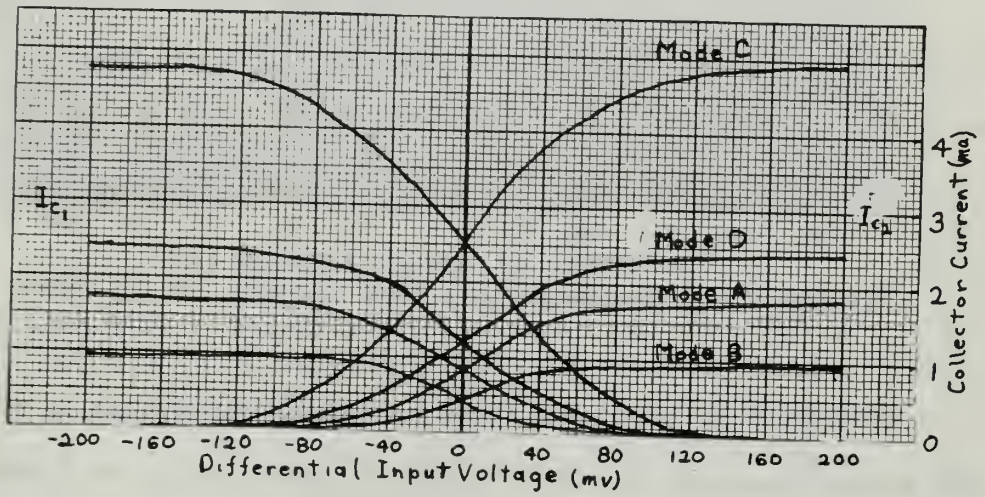

Figure 2.3: Transfer Curves of CA-3005

The transconductance of the differential pair is defined:

$$(7) \quad g_{m_1} = \frac{d(i_c)}{d(V_{b_1} - V_{b_2})}$$

Differentiating equations (6), we have the following equation for g_{m_1}.

$$(8) \quad g_{m_1} = \frac{\pm \alpha \frac{q}{kT} I_o \exp\left[\frac{q(V_{b_1} - V_{b_2})}{kT}\right]}{1 + \exp\left[\frac{q(V_{b_1} - V_{b_2})}{kT}\right]^2}$$

A plot of experimentally derived g_{m_1} versus differential input voltage is shown in figure 2.4 for several values of I_o.

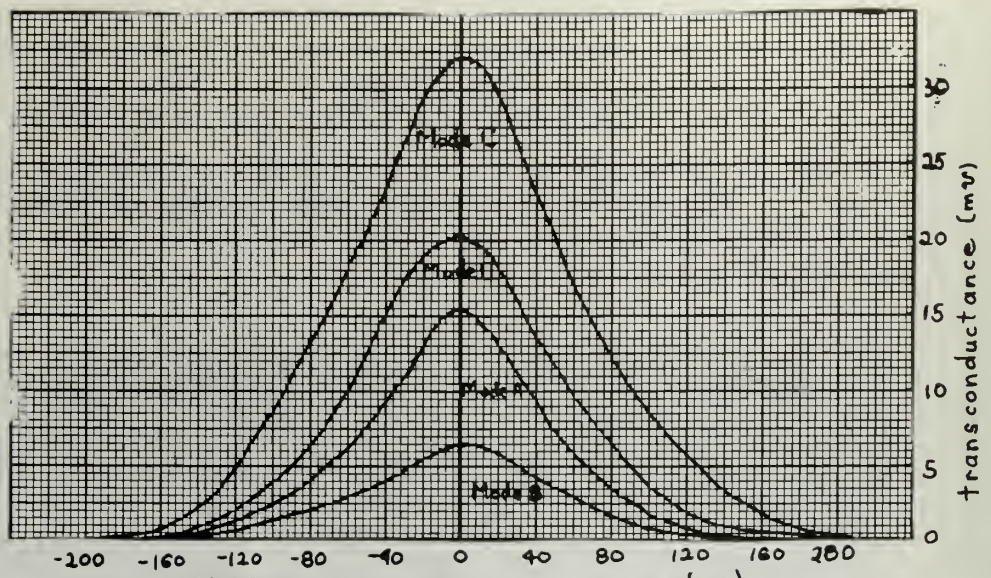

Figure 2.4: Transconductance Curves of CA-3005

The curves of figures 2.3 and 2.4 showed variations in transfer and transconductance of the differential pair with I_o as a parameter. We will now discuss the constant current-sink, Q_3, which controls I_o. The current sink is shown in figure 2.5a.

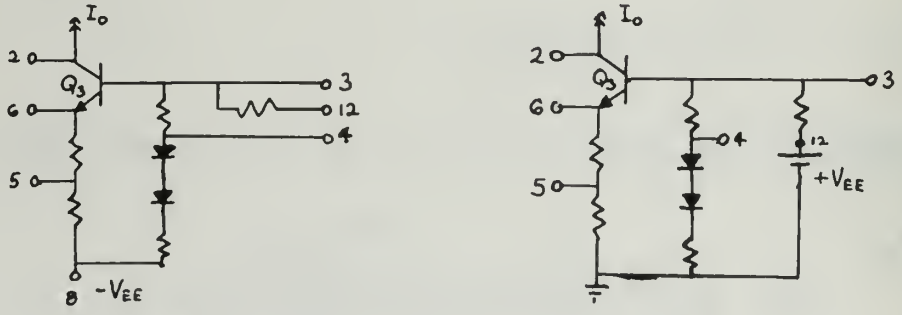

Figure 2.5: Schematic Diagram of Current Sink Q_3

Pin 12 is normally grounded and provides the base bias for Q_3. By shifting the supply voltage source and ground reference, we have, after redrawing in figure 2.5b, an equivalent circuit with Q_3 at the same operating point as in figure 2.5a. The current sink is

seen to be a standard common-emitter configuration with temperature compensation and stabilization. The analysis of this circuit is well covered in the literature[3]. This portion of the circuit not only provides the high AC-to-DC impedance ratio required for proper operation of the emmitter-coupled pair, but also provides another point for signal injection. I_o, the operating current for Q_1 and Q_2 can be controlled by applying a voltage to the base at pin 3.

In addition, the DC level of I_o can be set by the installation of jumpers between certain terminals. The RCA designations for these bias setting are defined below, together with measured I_o and maximum g_m values.

Current Mode	Connection (Pin Nos.)	I_o(ma)	g_m(m)
A	No Connection	3.8	15.5
B	4 shorted to 8	1.7	6.5
C	5 shorted to 8	9.4	32.1
D	4,5 shorted to 8	5.0	19.5

Figure 2.6 shows the transfer characteristics of Q_3, I_o versus V_{b_3}:

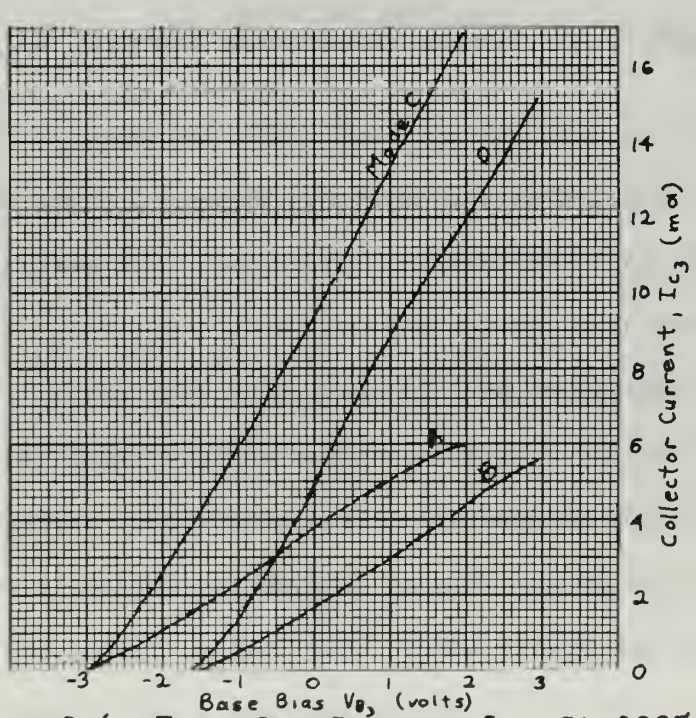

Figure 2.6: Transfer Curves, Q_3, CA-3005

The region of linear operation is well defined. A graph of small-signal transconductance is shown in figure 2.7. G_{m_3} is nearly constant through the linear region as would be expected. G_{m_3} is the rate of change of I_o with respect to V_{b_3}.

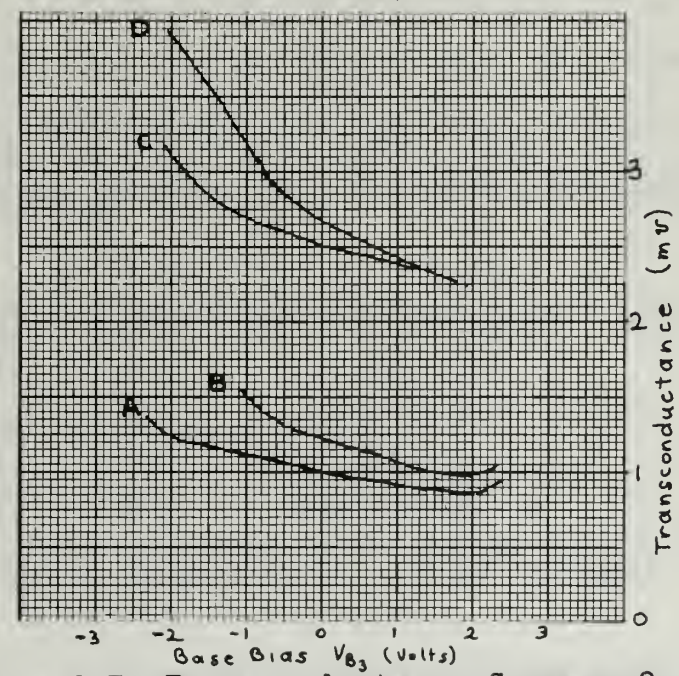

Figure 2.7: Transconductance Curves, Q_3, CA-3005

Some important features of the CA-3005 pertinent to this investigation are illustrated in the curves of figures 2.3 and 2.4.

(1) If the external circuit is balanced, the operating point occurs at $V_{b_1} - V_{b_2} = 0$, $I_{c_1} = I_{c_2}$, $I_{c_1} + I_{c_2} = I_o$.

(2) The transconductance is maximum at this point.

(3) The transfer curves are approximately linear only for a small portion of possible differential input voltages near the inflection point. The g_{m_1} curves are initially constant and then become square law in this region, indicating that the transfer curves rapidly change into a cubic form.

(4) Variations in I_o change the maximum value of g_{m_1} in each case, but the region described in (3) retains the same bounds for differential input voltage.

(5) One $(V_{b_1} - V_{b_2}) \rangle (\frac{kT}{q})$, the respective collector currents approach zero and I_o assymptotically. Maximum current in both transistors at any one time is I_o due to the constant current sink. (i.e., From equation (1) $\frac{I_{c_1}}{\alpha} + \frac{I_{c_2}}{\alpha} = I_o$ $I_{c_1} + I_{c_2} = \alpha I_o$. As I_{c_1} approached zero, I_{c_2} approaches I_o).

In summary, then, the distinctive operating regions on the g_{m_1} curves are (1) the constant-g_{m_1} region for small inputs about the operating point; (2) the square-law region near the operating point; (3) the linear region; and (4) another square-law region on near saturation or cutoff.

These characteristics, together with those already discussed in connection with Q_3 (figures 2.6 and 2.7), will be used to initially determine bias points and voltage levels in evaluating the mixing properties of the CA-3005.

3. Theory

Before further investigation of the CA-3005 characteristics, it would be well to discuss the modulation or mixing process in general. The frequency conversion process requires that some frequency or band of frequencies be translated to another region of the frequency spectrum. The frequencies to be translated will be referred to as the "AF" components while the carrier effecting the translation will be called the "LO" component, and the resulting translation will be the "RF" components. A mixer and a modulator perform similar functions and the process involved in the two functions are identical when performed in the manner to be here described. Since a linear device would by definition provide only the superposition of the LO and AF inputs, frequency translation is inherently a non-linear process.

Basically, this device can be used as a mixer in either of two ways. If the AF and the LO signal are added as an input to the differential pair with Q_1, Q_2 biased in a non-linear region, product terms will give rise to sum and difference frequencies resulting from the series expansion of the sum. The specific frequencies, in terms of the original AF and LO components contained in a given sum or difference term, depend on the degree of the polynomial approximation to the non-linearity. The amplitudes of the sum and difference frequencies depend on the form of the non-linearity and the relative amplitudes of the AF and LO components. For example, assuming a square law relation, we have:

$$(e_{AF}\cos\omega_{AF}t + e_{LO}\cos\omega_{LO}t)^2 = e_{AF}{}^2\cos^2\omega_{AF}t + 2e_{AF}e_{LO}\cos\omega_{AF}t\cos\omega_{LO}t$$

$$+ e_{LO}{}^2\cos^2\omega_{LO}t = \text{A.C. terms} + e_{AF}e_{LO}\cos(\omega_{AF} + \omega_{LO})t$$

$$+ e_{AF}e_{LO}\cos(\omega_{LO} - \omega_{AF})t + \text{D.C. terms}$$

Actually we see that the product term in the square-law expansion provides the desired frequency translation. This suggests that if the device output is a function of the product of two independently controllable variables, this product term should provide frequency translation. Equations (6) showed the output to be the product of I_o and some function of the differential input voltage. This is the second method of modulating or mixing. Both methods will be shown to be essentially the same in principle.

Redrawing one of the transfer curves from figure 2.3 we see that in the first method described above we vary the Q point from its offset DC value along the curve in a sinusoidal fashion, following the LO voltage, while the AF voltage, which is much smaller, varies about the moving Q point. The AF voltage is small enough so that the variation in g_{m_1} due to the AF voltage is negligible when compared to that caused by the LO voltage.

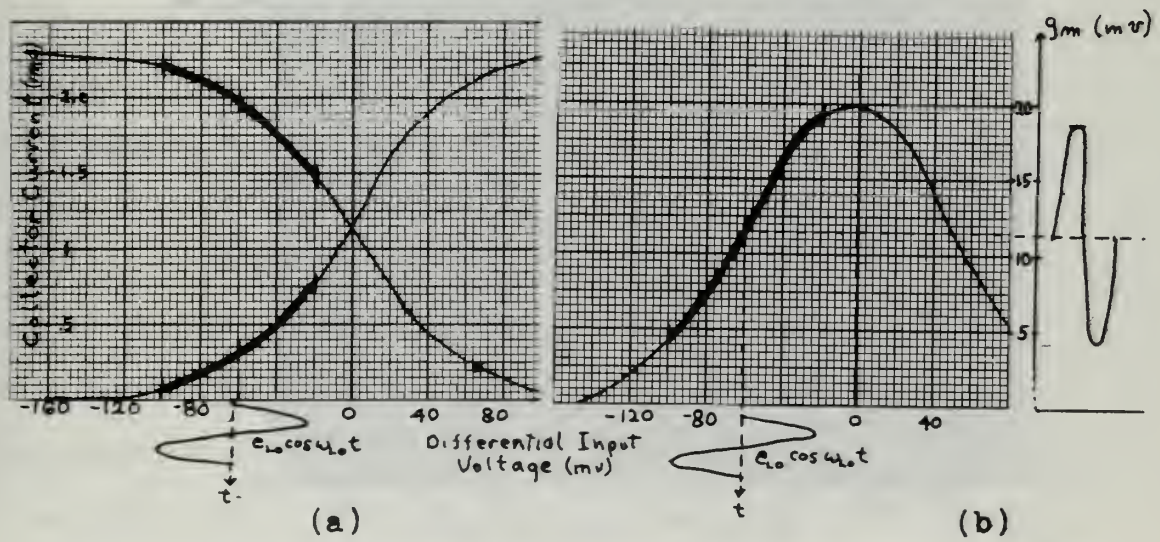

Figure 3.1: (a) Transfer Curves; (b) Transconductance illustrating operating point variation

In the case of figures 3.1 we have $g_m = f(e_{LO})$ and $e_{RF} = g_m R_L e_{in} = g_m R_L (e_{LO} + e_{AF})$. Assuming a linear relation between g_m (t) and $e_{LO}(t)$, we have the following result:

$$e_{RF} = g_m R_L [k_1 \cos\omega_{LO} t + k_2 \cos\omega_{AF} t]$$

$$= R_L [g_{m_g} + k_3 \cos\omega_{LO} t][k_1 \cos\omega_{LO} t + k_2 \cos\omega_{AF} t]$$

$$= \text{A.C. terms} + \frac{R_L k_3 k_2}{2} [\cos(\omega_{LO} + \omega_{AF})t$$

$$+ \cos(\omega_{LO} - \omega_{AF})t] + \text{D.C. terms}$$

Looking now at the second method discussed above, we will show that the translation process is the same as that of the first method. Transfer curves are shown in figure 3.2 for different values of Q_3 voltage level. Q_3 is biased in current mode D.

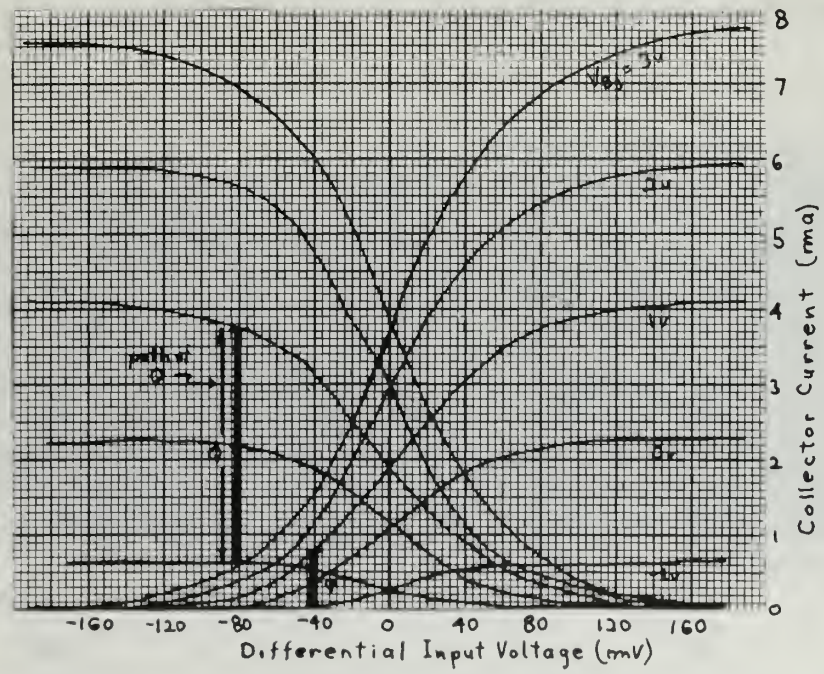

Figure 3.2: Transfer Curves for Selected Values of V_{b_3}

We see that the Q point rises and falls along the path shown, in accordance with the V_{b_3} voltage. Since the g_m for the AF signal is the instantaneous slope of these transfer curves on the Q path we see that the g_m varies in accordance with the voltage at V_{b_3}. Curves of transconductance versus differential input voltage are shown in figures 3.3 for various values of V_{b_3}, again with Q_3 in current mode D.

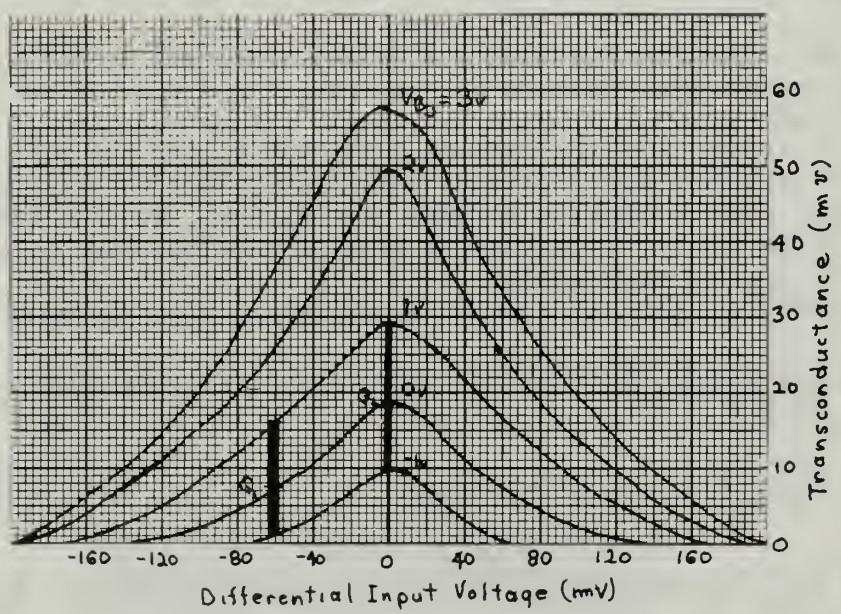

Figure 3.3: Transconductance Curves for selected values of V_{B_3}

In order to show more clearly the variation of g_m with time, the curves of figures 3.4 were plotted showing the g_{m_2} - versus - V_{b_3} relation for two different Q points as sketched in figures 3.3. G_{m_2} is the rate of change of output current with respect to the differential input $V_{b_1} - V_{b_2}$.

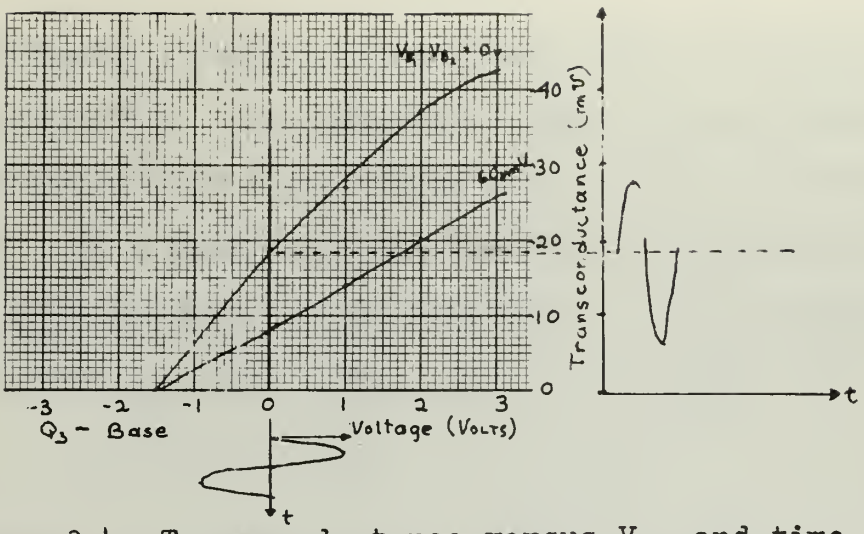

Figure 3.4: Transconductance versus V_{B_3} and time

Again we have the relation $e_o = g_m R_L e_{in} = g_m R_L e_{AF}$. Assuming, as before, a linear relation between $g_m(t)$ and $e_{LO}(t)$, we have the result below. The assumption is made that $e_{AF} \langle\langle e_{LO}$ so that variations in g_m due to e_{AF} are negligible.

$$e_{RF} = g_m R_L K_2 \cos\omega_{AF} t$$

$$= R_L[g_{m_Q} + k_3 \cos\omega_{LO} t] k_2 \cos\omega_{AF} t$$

$$= g_{m_Q} R_L k_2 \cos\omega_{AF} t + \frac{R_L k_3 k_2}{2}[\cos(\omega_{LO} + \omega_{AF})t + \cos(\omega_{LO} - \omega_{AF})t]$$

We see here that the sum and difference frequency terms, the terms of interest, are identical if the constant relating g_m to e_{LO} is the same in each case.

It is evident that the oscillator voltage should be made as large as possible in order to increase the conversion transconductance (i.e. the quotient of RF current at the desired frequency to AF input voltage). If the device is being used to amplitude modulate a LO signal by inserting the AF signal in Q_3, the amplitude of the AF signal should be limited to a value that would insure a linear relationship between I_D

and V_{b_3}. On the other hand, as a mixer with the LO signal at V_{b_3}, the amplitude can be increased for higher conversion transconductance without affecting the linearity of the AF signal at V_{b_1}, V_{b_2}. Discarding the linearity assumption will modify the form of the results in the two examples shown above. However it can easily be shown that the basic simularity between the methods still holds.

Choosing the DC-bias level of the CA-3005 essentially entails the choice of I_o. Even operating the differential pair with offset base voltages, as in figures 3.1, does not alter the I_o setting. For as was pointed out earlier, the sum of the base and collector currents in Q_1 and Q_2 is equal to I_o. Equations 6 and 8 indicate that the transconductance of the differential pair is proportional to I_o. This would seem to indicate that as high a level of I_o as can be tolerated should be used for this application. Curves showing the variation of g_{m_1} and g_{m_2} with power-supply voltage are shown in figure 3.5 below.

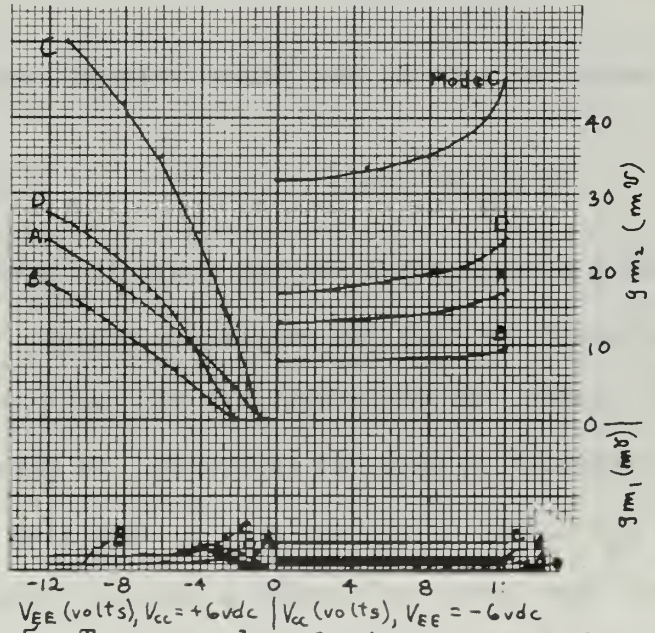

Figure 3.5: Transcondconductance as a function of Power Supply Voltage

For these measurements, one supply voltage was held constant at $\pm$ 6 VDC while the other was varied from zero to $\pm$ 12 VDC and g_m measured. 18 VDC is the specified maximum voltage drop permitted between pins 9 and 8. These curves show that g_{m_2} is constant with change in I_o, as long as there is a current path from pin 9 to pin 8. G_{m_1} is not sensitive to variations in I_o until the differential pair approaches saturation. The curves do show explicitly the dependence of g_{m_1} on I_o, or Q_3 biasing. One would conclude from the foregoing that Mode C should be chosen with

$$V_{EE} = -12VDC \qquad \text{and} \qquad V_{CC} = +6VDC$$

as the most promixing arrangement. However, experiments show that the differential pair is very close to saturation in Mode C for the higher supply voltage levels so that resutls are not very predictable or reliable. Mode D was chosen for this series of tests as being the next best possibility. Also,

$$V_{CC} = +6VDC$$

was chosen to permit as wide as possible a voltage swing at the collectors.

$$V_{EE} = -6VDC$$

was chosen since a more negative voltage would again drive Q_1, Q_2 to an operating point too near the saturation region.

Once I_o is chosen, the adjustments to the operating points can be made by the addition of external resistors. As previously stated, offset bias of Q_1, Q_2 may be accomplished by inserting a resistor in one of the input base leads, or inserting unequal resistors in each of the base leads. Q_3 is biased normally be grounding pin 12. A resistor added in series with lead 12 will lower the bias level,

while one placed in parallel with pin 12, (i.e. between pins 12 and 3). will raise the bias level of Q_3. All of these bias levels, however, are derived from the set level of I_o in conjunction with the supply-voltage levels.

4. Experimental Results

4.1 Discussion

The experimental portion of this investigation is written in two sections. The first deals with insertion of both LO and AF signals into the differential pair. Different portions of the transconductance curve of figure 2.4 are used either singly or together, depending on the results expected from inspection of the curve shape. The results are compared in terms of conversion gain and distortion and inter-modulation effects.

As discussed earlier in this paper, the processes involved in mixing or amplitude modulating are the same. Since using more than one frequency for the AF signal (i.e. an AM modulated wave, for example) would unnecessarily complicate the experiment, all data were taken using a 10-Khz sinusoidal wave for the LO signal, and a single 500-Hz sinusoidal wave for the AF signal. For this reason, any distinction between mixing and modulating in this portion of the experiment is academic.

Since the purpose of a frequency translator is to shift a band of frequencies higher or lower in the frequency spectrum, the process used must not distort the relative amplitudes of the components within the band. The contributions to non-linear distortion of the shifted frequencies were evaluated for each of the methods studied.

There are actually two features of the characteristics curves that come under consideration. Ideally, the translated AF signal should contain the same frequency components as the input AF signal, with the same relative amplitudes. Deviations from this ideal are primarilly due to the following reasons: (1) Harmonics of the

individual input components may occur as a result of the deviation of the device characteristics from linearity with respect to the AF signal, with or without a LO signal applied. This can be evaluated by looking at the CA-3005 as a three-terminal device and ignoring the other input terminal. With proper mixing characteristics, the device should still retain linearity even with a LO signal applied. (2) If the device characteristics indicate strong cubic effects, the mixing process may produce additional frequency components within the translated spectrum of the AF signal.

Two measures of distortion were applied. One, using a single AF component, measured harmonic distortion as a percentage of the fundamental AF component[4] in the output. This measurement was made of components about the fundamental LO frequency, except in Method III, where the measurements were made at the second harmonic of the LO frequency. The second method used was an intermodulation method[5] in which two equal sine waves were used as the input AF signal. These signals were spaced relatively close to each other so that their difference frequency would be observed easily, if distortions in the process produced it.

Frequency conversion, as considered in this paper, may be regarded as basically a process of modulating the LO frequency by the AF frequency. Since in a practical case the AF component would be very much smaller than the LO component of collector output current, the percentage modulation would be very small. For this reason, higher-order non-linear effects may be neglected in the process. That is, g_m is a function of the LO alone. As is well known, the amplitude of one of the sidebands is one half the modulation index times the carrier amplitude. Expanding g_m into a Fourier series, we have:

$$(9)\quad g_m = a_o + a_1\cos\omega_{LO}t + a_2\cos 2\omega_{LO}t + \ldots\ldots$$

The cosine series can be used since as illustrated in figures 3.1 and 3.4, g_m is a single-valued function of the LO signal which varies as $\cos\omega_{LO}t$. Applying a small signal, $e_{AF}\cos\omega_{AF}t$, to the device the resulting collector current is as follows.

$$(10)\quad i_c = g_m e_{AF}\sin\omega_{AF}t = e_{AF}\sum_{n=1}^{\infty} a_n \sin\omega_{AF}t\cos n\omega_{LO}t$$

$$(11)\quad i_c = a_o e_{AF}\sin\omega_{AF}t + \frac{1}{2}e_{AF}\sum_{n=1}^{\infty} a_n \sin(\omega_{AF} + n\omega_{LO})t + \frac{1}{2}e_{AF}\sum_{n=1}^{\infty} a_n \sin(\omega_{AF} - n\omega_{LO})t$$

filtering at the output of the device selects any of the frequencies $\omega_{AF} \pm n\omega_{LO}$ which are the RF components. Since conversion transconductance is the ratio of the desired output current component to the signal input voltage, we have from equation 11, the following.

$$(12)\quad g_{c_n} = \frac{i(\omega_{AF} \pm n\omega_{LO})}{e_{AF}} = \frac{a_n}{2}$$

Then evaluating g_{c_n} from (9) and (12) we have:

$$(13)\quad g_{c_n} = \frac{1}{2\pi}\int_o^{2\pi} g_m \cos n\omega_{LO}t\,(d\omega_{LO}t)$$

Most small-signal devices for use as mixers have g_m characteristics that produce the largest Fourier coefficients at the fundamental, with rapidly decreasing higher-order harmonic coefficients thereafter.

The experimental data gathered for the first five examples was checked against calculations using a graphical method of harmonic analysis due to Chaffee[6]. Formulae used for the fundamental and first two harmonics were[7]:

(14)

$$g_{c_1} = \frac{1}{12}[(g_7 - g_1) + (g_5 - g_3) + 1.73(g_6 - g_2)]$$

$$g_{c_2} = \frac{1}{12}\left[2g_4 + \frac{3}{4}(g_3 + g_5 - g_6 - g_2) - (g_7 + g_1)\right]$$

$$g_{c_3} = \frac{1}{12}[(g_7 - g_1) - 2(g_5 - g_3)]$$

A sample calculation using (14) is contained in Appendix I and the computed values of g_{c_n} are compared with experimental values. The method gives good results for the fundamental and second harmonics but the third harmonic is a poor approximation.

4.2 Method I

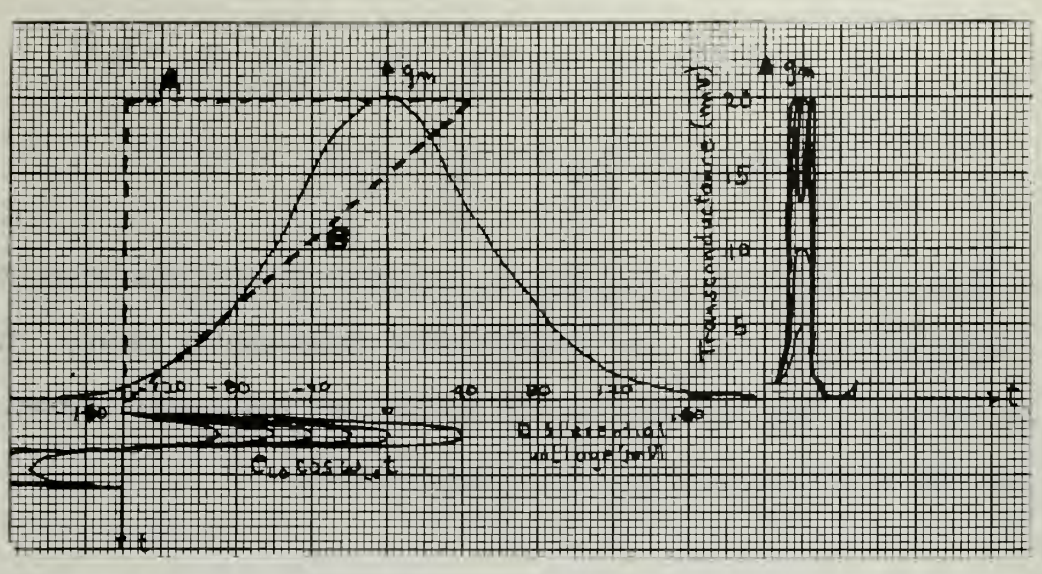

Figure 4.1: Graphical Illustration of Method I with Large Offset Bias

In this method, one of the transistor output pair is biased near cutoff and the other near saturation. The positive-going peak of the LO signal pushes both Q_1 and Q_2 toward the maximum transconductance region. Inspecting the bounds of the transconductance in conjunction with equation (13) indicates the the maximum conversion gain possible with any device in this condition of bias is represented by the dotted curve "A". This would give $g_{c_{max}} = g_{m_{max}}/\pi$, or one half of the integrated value, since the device operates only half a period. The negative cosine values would subtract from the integral over a time period, thereby reducing $g_{c_{max}}$. This would indicate the bias point should be very nearly at cutoff. Curve "C" shows the minimum value to be expected, and for the positive half cycle only, can be shown from (13) to be nearly one fourth $g_{m_{max}}$. The above bounds on g_c refer to the fundamental component (n = 1).[8]

A plot of conversion gain versus LO injection voltage is shown in figure 4.2 for the fundamental and second harmonic.

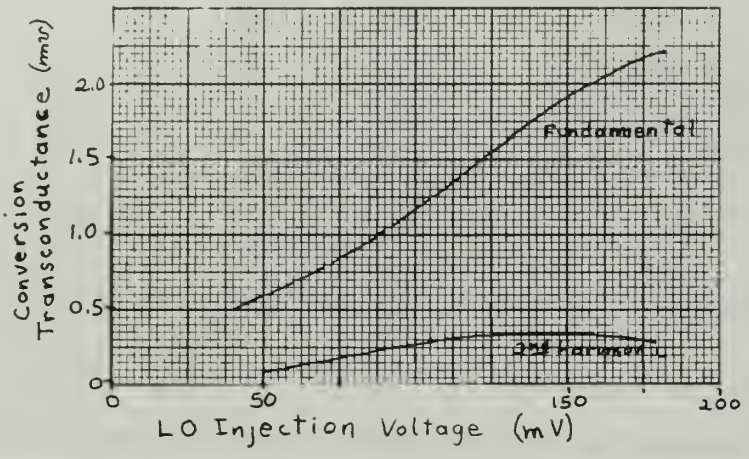

Figure 4.2: Variation of Conversion Transconductance with LO Injection Voltage: Method I

We see that conversion gain increases linearly with LO injection until the LO peak exceeds the maximum value of transconductance. The expected value of approximately one fourth the maximum transconductance is not reached because of the existence of higher-order harmonics. The rate of increasing conversion transconductance begins to fall off once the peak of the cosine reaches maximum g_m, since beyond this point there is a sharp dip in the g_m - versus - time curve of figure 4.1.

Shown in figure 4.3 is a plot of distortion and intermodulation plotted against LO voltage amplitude. Both effects remain relatively constant although the trend indicates large LO voltages are desireable.

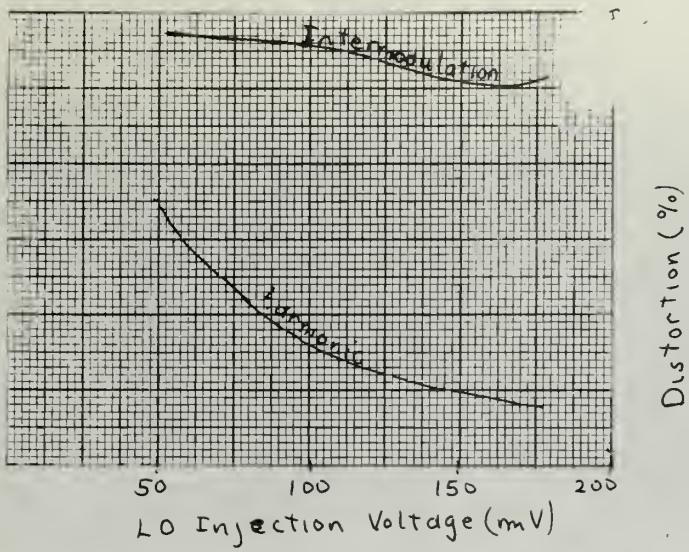

Figure 4.3: Distortion and Intermodulation versus LO Voltage: Method I

4.3 Method II

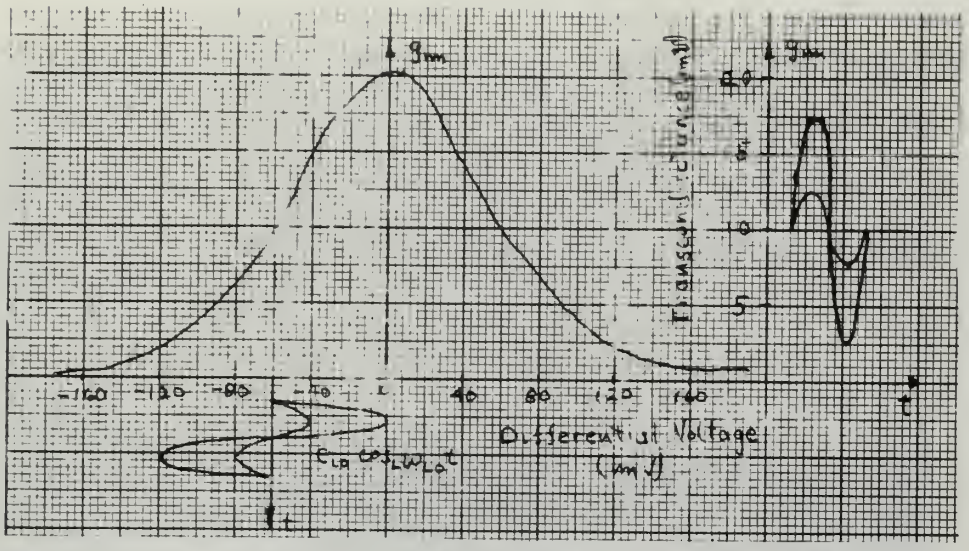

Figure 4.4: Graphical Illustration of Method II with Offset Bias

Since the bias point places the variations in g_m near the maximum region of the transconductance curve for a greater period of time, the conversion transconductance is expected to be higher. Figure 4.5 shows a plot of co version transconductance versus LO injection voltage.

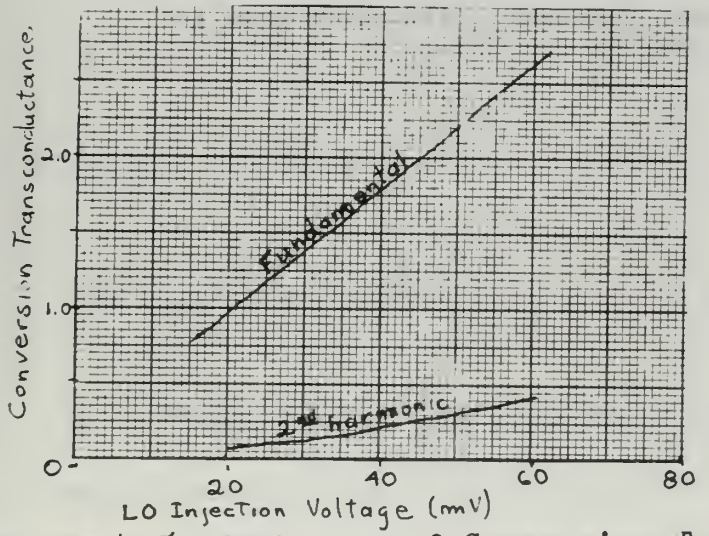

Figure 4.5: Variation of Conversion Transconductance with LO Injection Voltage: Method II

Again, the conversion gain is a linear function of the LO injection voltage throughout the range tested.

Figure 4.6 shows a plot of distortion and intermodulation effects plotted against LO injection voltage. Here, the intermodulation effects are relatively constant. The harmonic distortion falls sharply with increase in LO injection voltage to a low value.

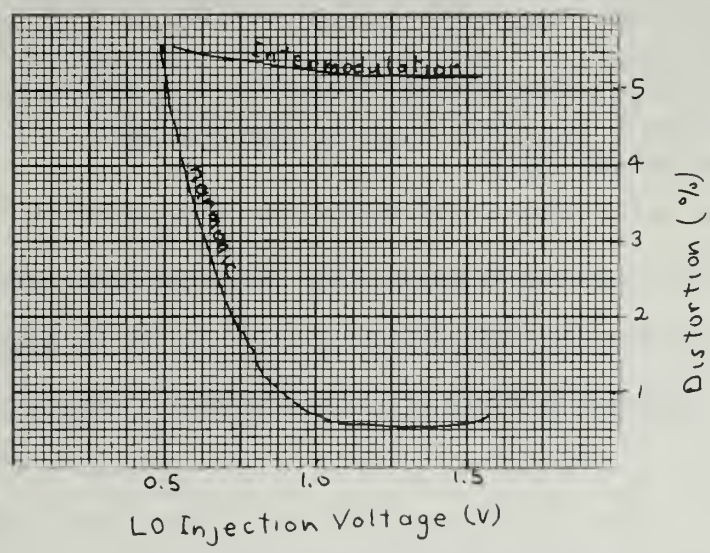

Figure 4.6: Distortion and Intermodulation versus LO Voltage: Method II

4.4 Method III

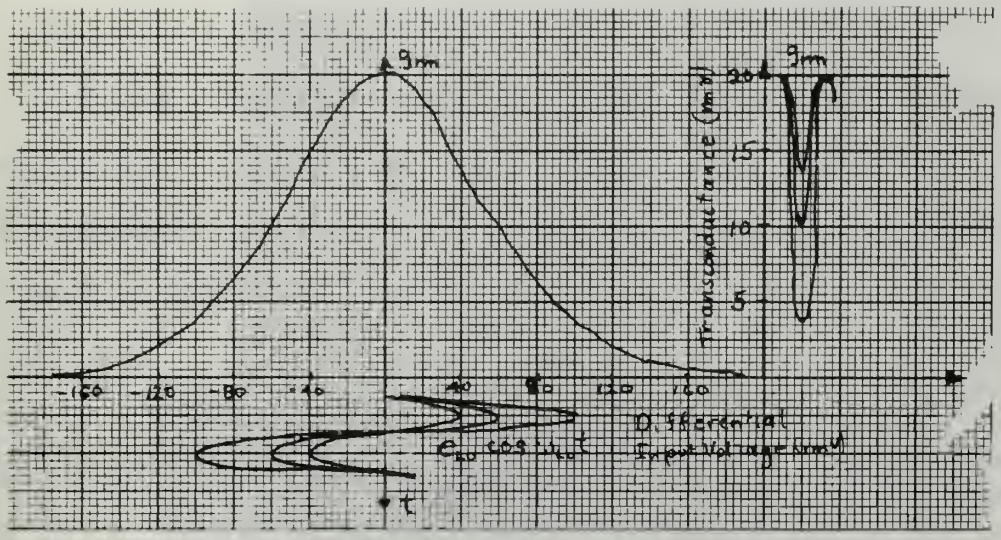

Figure 4.7: Graphical Illustration of Method III with Zero Offset

This method takes advantage of the symmetry of the g_m curve. From equation (8) we have

$$(8)\quad g_m = \frac{\alpha \frac{q}{kT} I_o \epsilon^{q\frac{(V_{b_1} - V_{b_2})}{kT}}}{\left[1 + \epsilon^{\frac{(V_{b_1} - V_{b_2})}{kT}}\right]^2} = \frac{k_1 k_2 I_o \epsilon^{k_2 V_{in}}}{\left[1 + \epsilon^{k_2 V_{in}}\right]^2}$$

And since I_o is a constant in this method of modulation, we have:

$$(15)\quad g_m = \frac{k}{2} I_o \frac{1}{1 + \cosh KV_{in}}$$

$$\text{where } V_{in} = e_{AF}\cos\omega_{AF}t + e_{LO}\cos\omega_{LO}t$$

The output current is $g_m V_{in}$, an even function of the input voltage. A plot showing the conversion gain versus LO injection voltage is shown in figure 4.8

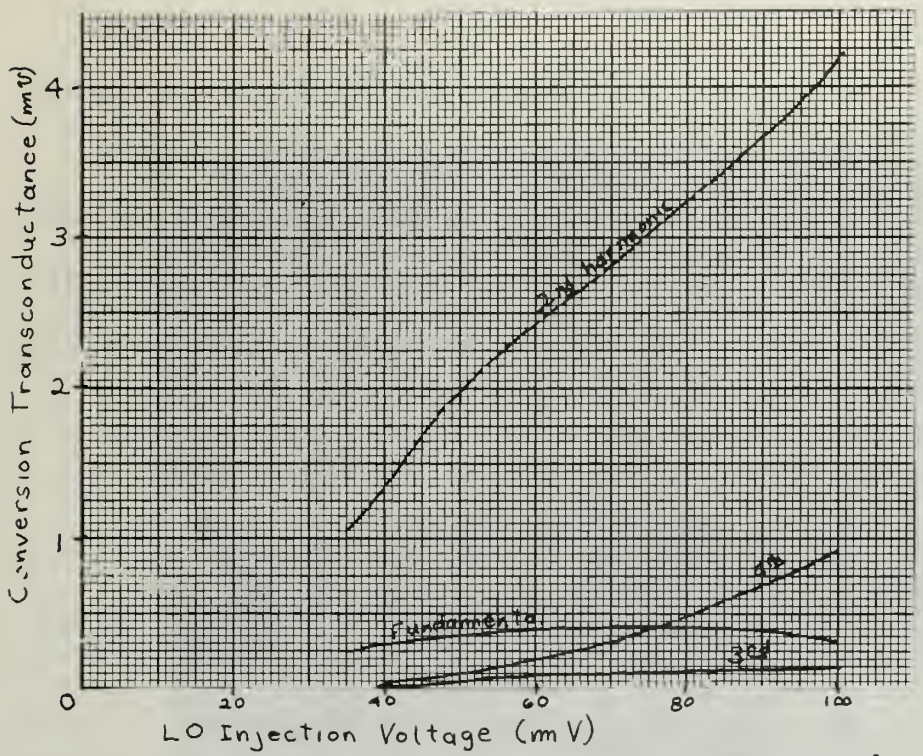

Figure 4.8: Variation of Conversion Transconductance with LO Injection Voltage: Method III

We see that once the LO voltage becomes sufficiently large, the second harmonic and fourth harmonic increase linearly with LO input voltage. The existence of odd-order harmonics is due to deviations in the actual circuit used from the ideal, symmetrical case. The device transconductance curve must be perfectly symmetrical since deviations from symmetry will cause different values of g_m for positive and negative excursions of the LO cosine wave. More important, there must be no offset either from internal device imbalances or from the external circuit. It can be seen in figure 4.7 that a slight shift of this bias point will create a positive swing of the g_m versus time curve over the quiescent value.

This bias condition is interesting because it enables one to

design a converter circuit with the oscillator operating at one half the frequency required in a normal, first-order conversion process, while obtaining reasonably high values of transconductance.

Figure 4.9 below shows a plot of intermodulation distortion and harmonic distortion as a function of LO voltage amplitude. Intermodulation distortion is relatively constant while harmonic distortion falls with increasing LO voltage.

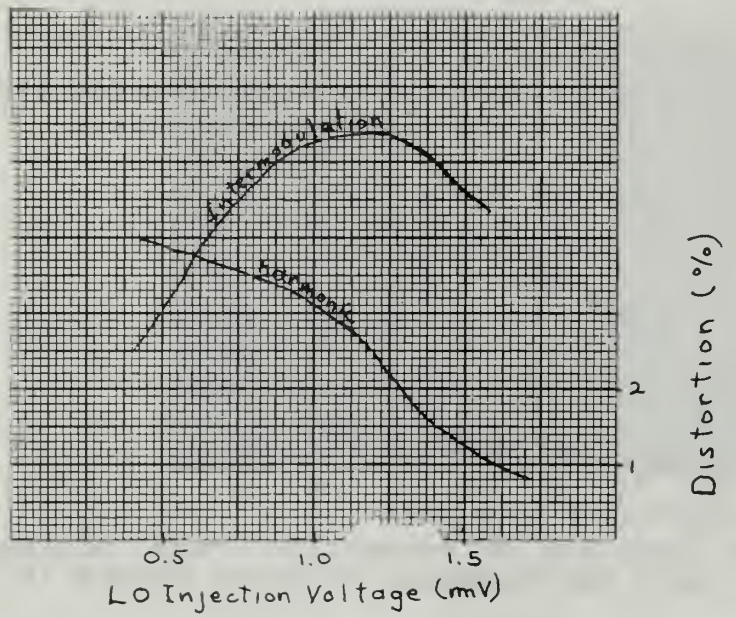

Figure 4.9: Distortion and Intermodulation versus LO Voltage: Method III

4.5 Method IV

In Method IV, the AF signal input is to the differential pair, while the LO signal is injected into the base of the constant-current sink. Figure 3.3 illustrates the operation of the device where the operating path is that of Q_2. In calculating the conversion gain g_{c_n} for the first three frequency components, figure 3.4 with $V_{B_1} - V_{B_2} = 0$ was used. Figure 4.10 shows a plot of conversion gain versus LO injection voltage.

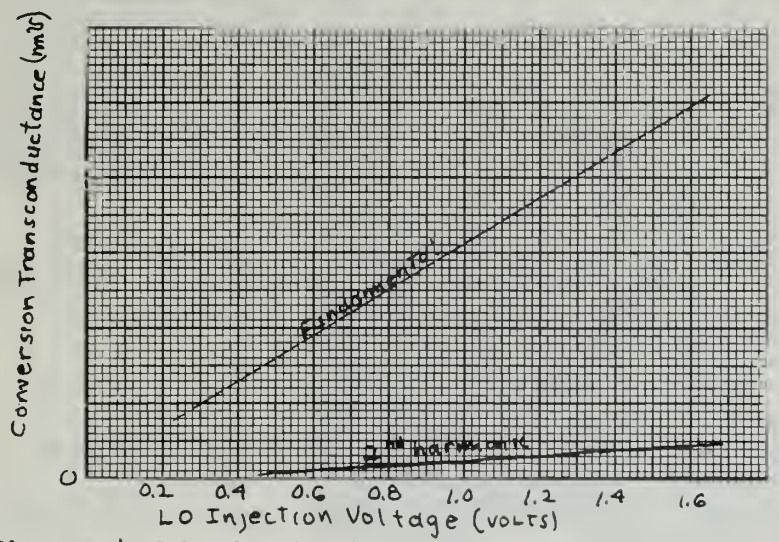

Figure 4.10: Variation of Conversion Transconductance with LO Injection Voltage: Method IV

These curves indicate nearly linear change in conversion gain with LO injection voltage. This performance is expected from an inspection of the curves of figure 3.4. It is also apparent that a linear approximation to g_m would be reasonably accurate here. That is, $g_m = 19.5 + 11\, e_{LO} \cos\omega_{LO} t$.

The intermodulation and harmonic distortion characteristics are plotted in figure 4.11 as a function of LO voltage amplitude. It is seen that both functions stay fairly constant as LO voltage increases.

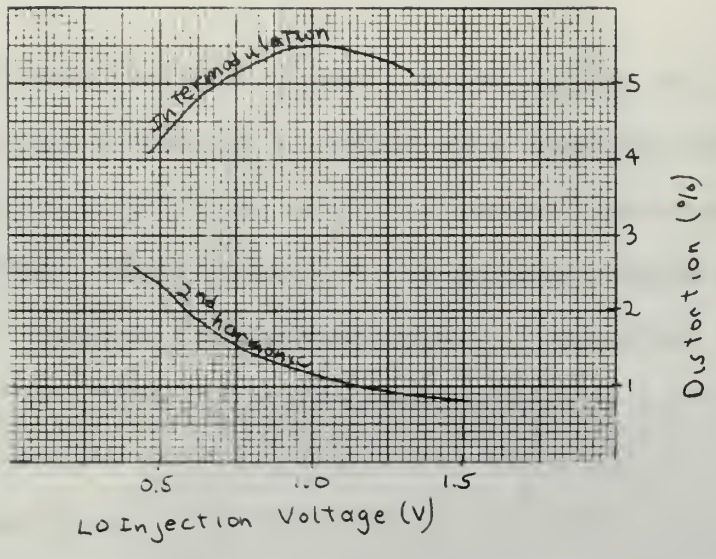

Figure 4.11: Distortion and Intermodulation versus LO Voltage: Method IV

4.6 Method V

This method is the same as Method IV except that the differential pair is biased offset from zero. The curves of figure 3.3 again describe the operation of the device with the operating point following the path of Q_1. Figure 4.12 shows the variation of conversion gain with LO injection voltage for this method. The offset used was 60 mv.

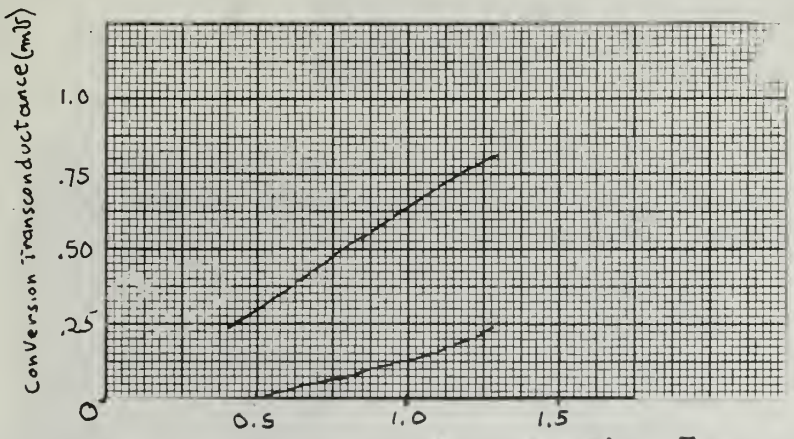

Figure 4.12: Variation of Conversion Transconductance with LO Injection Voltage: Method V

A plot of intermodulation and harmonic distortion is shown in figure 4.13. This plot is not vastly different from that of 4.11 except that the upward trend of the intermodulation curve indicates increasing non-linearity in the g_m variations with LO voltage.

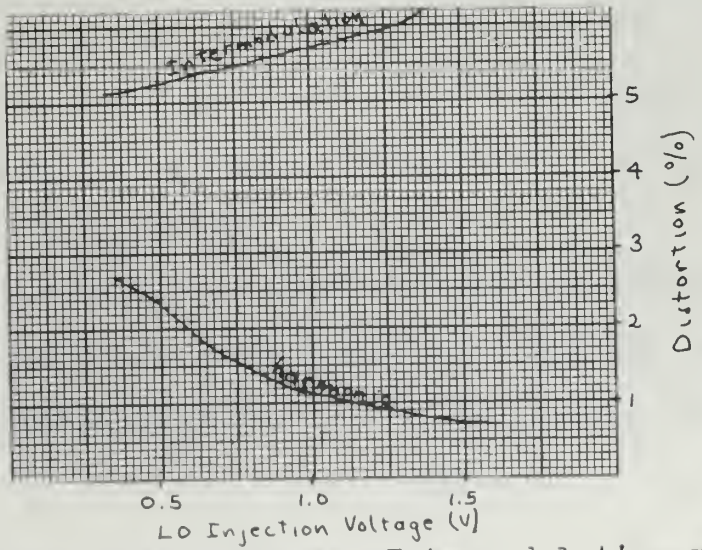

Figure 4.13: Distortion and Intermodulation versus LO Voltage: Method V

4.7 Method VI

In Method VI the AF signal is injected in the base of the constant-current sink while the LO signal input is fed into the differential pair. Again figures 3.3 and 3.4 illustrate the operation of the device. In order to obtain reasonably high conversion gains, the voltage levels of both inputs are required to be relatively large. LO injection used was 100 mv., while AF voltage was varied from 0.5 to 1.5 volts peak. The assumption made in previous methods that g_m was a function of the LO signal alone is no longer valid. The analysis must be altered to account for this change in method. Now we have the condition:

$$(16) \quad i_c = g_{m_1}' (V_{b_1} - V_{b_2}) + g_{m_2}' V_{b_3} + \text{other term}$$

Curves in figures 2.4 and 3.4 show g_{m_1} and g_{m_2}, respectively. Since each of these transconductances is a function of both the differential input voltage and the constant-current sink input voltage, a detailed analysis would be quite complicated. The last term fails to provide a product term and will be ignored. If we also ignore the non-linearity at each injection point, however, the transconductance from one injection point to the collector can be approximated as a function of the instantaneous bias on the other. That is, $g_{m_1}' = f_1(V_{b_3})$ and $g_{m_2}' = f_2(V_{b_1} - V_{b_2})$. Then equation (16) becomes:

$$(17) \quad i_c = [f_1(V_{b_3})] (V_{b_1} - V_{b_2}) + [f_2(V_{b_1} - V_{b_2})](V_{b_3}) + \text{other terms}$$

Each term can now be treated as in the previous methods. The coefficients of like frequencies in each term are added to give the result. Calculations using this method indicated reasonably close agreement with experimental values. An example is worked in Appendix I.

Plots of conversion transconductance versus AF injection voltage are shown in figure 4.14. The gain is constant with variation in AF voltage and is low. This is expected from figure 2.7

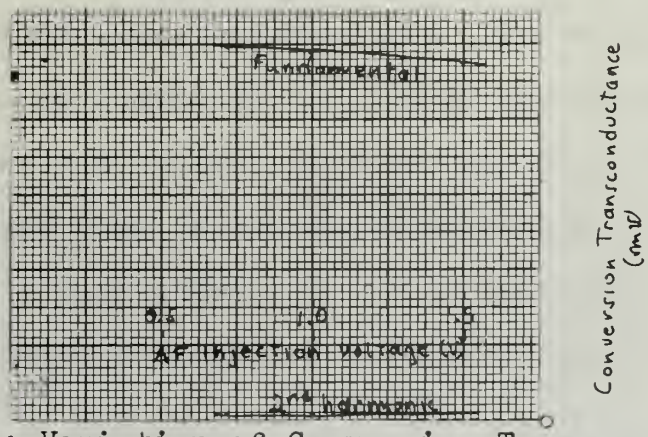

Figure 4.14: Variation of Conversion Transconductance with LO Injection Voltage: Method VI

Next is shown a plot of intermodulation and harmonic distortion as a function of AF voltage.

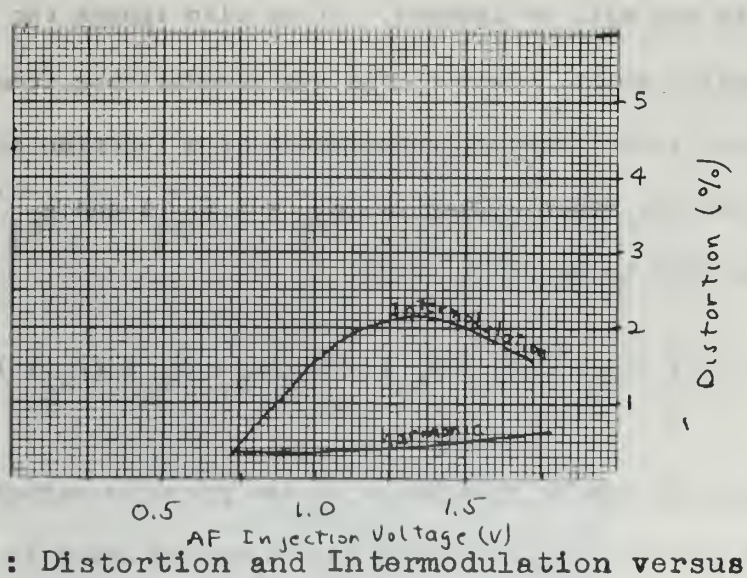

Figure 4.15: Distortion and Intermodulation versus LO Voltage: Method VI

4.8 Method VII

This method is identical to Method VI except for the DC offset of the differential pair. The plot of conversion gain versus AF voltage is shown in figure 4.16. Again these values are a constant function of AF voltage.

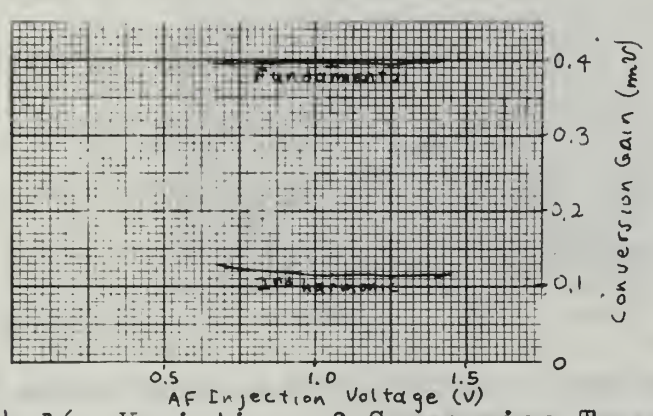

Figure 4.16: Variation of Conversion Transconductance with AF Injection Voltage: Method VII

Shown in figure 4.17 are the intermodulation and harmonic distortion characteristics for this method. Again, as in figure 4.13 we see the effect of the non-linearity of spacing between successive g_m lines in figure 3.3. This time, the harmonic distortion increases with increasing AF voltage because of the reversal of injection terminals between LO and AF.

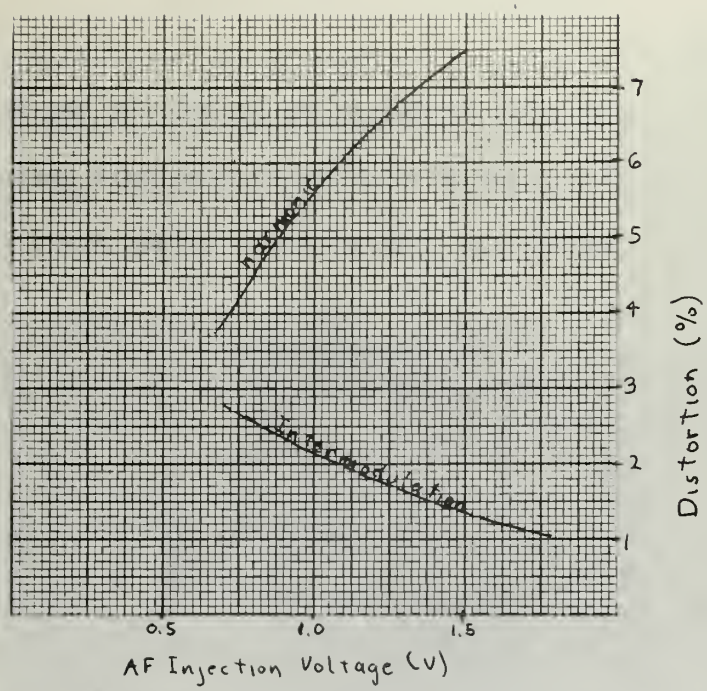

Figure 4.17: Distortion and Intermodulation versus LO Voltage: Method VII

5. Conclusions

The curves of the preceding section provide information which will permit the designer to anticipate the performance of the CA-3005 and similar devices in various operating configurations.

In Methods I, II, III, where both LO and AF signals are injected into the differential input, it is apparent that the choice of an operating point near the maximum g_m region is desireable. For translations to the fundamental of the LO signal, operation in the linear region of the g_m curve is preferred, while operation at zero offset would be appropriate for translation to the second harmonic of the LO signal. The conversion transconductances obtained compare favorably with other devices using similar methods of frequency conversion.

The distortion curves indicate that high values of LO injection voltage increase the desired RF component in amplitude more than the undesired harmonic components. That is, large ratios of LO to AF signal levels insure that g_m is a function of the LO signal rather than the AF and LO signal combined. Both the intermodulation and the harmonic distortion levels remain within acceptable bounds throughout the range of LO levels tested.

In the Methods IV and V, where the LO signal controls I_o and the AF signal controls the differential pair, we see that the levels of conversion gain are generally higher than those in the first method for the zero-bias condition. Offset bias provides no observable advantages over the zero-bias condition so will not be considered further. Again, intermodulation distortion remains relatively constant while harmonic distortion is reduced by increasing LO signal level.

Methods VI and VII, in which the AF signal was used to control I_o while the LO signal controlled the differential pair, provided relatively low conversion transconductances. The distortion and intermodulation effects in Method VII, with Q_1, Q_2 bias offset, were particularly poor, while those of Method VI were fairly good.

In general, the LO signal should be very much larger than the AF signal to obtain high conversion transconductances and low distortion levels. In using LO control of I_o, the best overall results are obtained.

All of the data was measured with a small load resistor in series with the supply voltage. Identical loads were inserted in each collector lead of the differential pair in order to maintain balanced characteristics and control DC offset at the base leads of the pair. Then with a transformer load, the results for distortion would remain essentially the same except for the effect of load impedance variations with frequency, and the conversion transconductances would be twice those listed in the experimental section.

Furthermore, with a balanced transformer output, the large LO component can be reduced to a level below that of the desired sidebands when using Method IV. This is important since conversion transconductance is proportional to LO injection voltage. The large LO drive requirements for this method cause large values of the carrier component to appear in the output. With a center-tapped primary, the LO component can be made to cancel out, to a degree depending on both the device and the circuit imbalances. Complete suppression of the carrier is limited by the device tolerances.

FOOTNOTES

[1]RCA, Inc., "Application of the RCA CA-3004, CA-3005 and CA-3006 Integrated-Circuit RF Amplifiers", RCA Electronics Components and Devices Div., Application Note ICAN - 5022, (Feb. 1966).

[2]RCA, Inc., Linear Integrated Circuit Fundamentals, Technical Series IC-41, RCA Electronic Components and Devices Div., Harrison, N. J., 1967, pp. 28-72.

[3]F. C. Fitchen, Transistor Circuit Analysis and Design, Van Nostrand, N. Y., 1966, p. 264.

[4]F. T. Terman, J. M. Pettit, Electronic Measurements, McGraw-Hill, N. Y., 1952, pp. 334-335.

[5]Ibid., pp. 338-340.

[6]E. L. Chaffee, "A Simplified Harmonic Analysis", Rev. Sci. Instr., Vol. 7, (Oct. 1936), pp. 384-389.

[7]E. W. Harold, "The Operation of Frequency Converters and Mixers for Superheterodyne Reception", Proc IRE, Vol. 30, No. 2, (Feb. 1942), pp. 84-103.

[8]C. F. Nesslage, E. W. Harold, W. A. Harris, "A New Tube for Use in Superheterodyne Frequency Conversion Systems", Proc.IRE, Vol. 24, No. 2, (Feb. 1936), pp. 207-215.

BIBLIOGRAPHY

A. BOOKS

Clifford, H. E. and Wing, A. H., Electronic Circuits and Tubes, (Cruft Laboratory, Electronics Training Staff), McGraw-Hill, N. Y., 1947, 994 pp.

Fitchen, Franklin C., Transistor Circuit Analysis and Design, Van Nostrand, N. Y., 1966, 412 pp.

Giles, James N., Fairchild Semiconductor Linear Integrated Circuit Applications Handbook, Fairchild Semiconductor Corp., Mountain View, Calif., 1966, 188 pp.

Lynn, D. K., C. S. Meyer, D. J. Hamilton, Analysis and Design of Integrated Circuits, McGraw-Hill, N. Y. 1967, 491 pp.

Middlebrook, R. D., Differentail Amplifiers, Weley & Sons, N. Y., 1963, 115 pp.

RCA, Inc., Linear Integrated Circuit Fundamentals, Technical Series IC-41, RCA Electronic Components and Devices Div., Harrison, New Jersey, 1967, 352 pp.

Terman, F. T., Electronic and Radio Engineering, McGraw-Hill, N.Y., 1955, 707 pp.

Terman, F. T., J. M. Pettit, Electronic Measurements, McGraw-Hill, N. Y., 1952, 707 pp.

Tucker, D. G., Modulators and Frequency Changers, MacDonald, London, 1953, 232 pp.

Tucker, D. G., Circuits and Periodically-Varying Parameters, Van Nostrand, London, 1964, 175 pp.

B. PUBLICATIONS OF THE GOVERNMENT, LEARNED SOCIETIES, AND OTHER ORGANIZATIONS

Botow, R., "Breadboard Techniques for Low Frequency Integrated Circuit Feedback Amplifiers", Motorola Semiconductor Products, Inc., Application Note AN-271 (n.d.).

Cummins, Earl L., "Overloading and Supurious Responses in Transistor FM Tuners", Fairchild Semiconductor Corp., Application Note TP-24, (Nov. 1963).

Estep, G. J., "Designing with the uA703 Monolithic RF-IF Amplifier," Fairchild Semiconductor Corp., Application Note APP-156, (May 1967).

McKeon, E. F., "Cross-Modulation Effects in Single-Gate and Dual-Gate MOS Field Effect Transistors", RCA Electronic Components and Devices Div., Application Note AN-3435 (Aug., 1967.

RCA, Inc., "Application of the RCA CA-3004, CA-3005 and CA-3006 Integrated-Circuit RF Amplifiers", RCA Electronic Components and Devices Div., Application Note ICAN-5022, (Feb. 1966).

Robertson, J.J., B. Welling, "An Integrated Circuit RF-IF Amplifier", Motorola Semiconductor Products, Inc., Application Note AN-247 (n.d.).

Robertson, J.J., "Tunded Amplifier Design with an Emitter-Coupled Integrated RF Amplifier", Motorola Semiconductor Products, Inc., Application Note AN-203 (n.d.).

Seymour, R., "A Monolithic RF/IF Amplifier and Its Applications", IEEE WESCON Conv. Record, Vol. 11, Part 2, 1967, pp. 1-10.

C. PERIODICALS

Chaffee, E. L., "A Simplified Harmonic Analysis", Rev. Sci. Instr., Vol. 7, (Oct. 1936), pp. 384-389.

Herold, E. W., "The Operation of Frequency Converters and Mixers for Superheterodyne Reception:, Proc. IRE, Vol. 30, No. 2, (Feb. 1942), pp. 84-103.

Keller, J. P., "Linear IC's: Part 3 - Differential Amplifiers at Work", Electronics, Vol. 40, No. 19, (Sept. 18, 1967) pp. 96-105.

Nesslage, C. F., E. W. Harold, W. A. Harris, "A New Tube for Use in Superheterodyne Frequency Conversion Systems", Proc. IRE, Vol. 24, No. 2, (Feb. 1936), pp. 207-215.

Robertson, S. T., "Designing an Integrated Differential Amplifier", Electrical Design News, (June 1965), pp. 34-41.

Widlar, R. J., "Some Circuit Design Techniques for Linear Integrated Circuits", IEEE Transactions on Circuit Theory, Vol. CT-12, No. 4, (Dec. 1965), pp. 586-590

Zawels, Jakob, "The Transistor as a Mixer", Proc. IRE, Vol. 42, No. 3, (Mar. 1954), pp. 542-548.

Appendix I

Sample Calculation Using Chaffee's Method of Harmonic Analysis

The sample calculation performed in this appendix will serve the dual purpose of illustrating the applicability of Chaffee's method of harmonic analysis to the transconductance curves of this device and will show the usefullness of the approximation made in the analysis of Methods VI and VII in which the variation of transconductance with time is a function of two independent voltage inputs.

Previously we had the relation developed in the experimental section for Method VI that:

$$i_c = [f_1(V_{b_3})] (V_{b_2} - V_{b_1}) + [f_2(V_{b_1} - V_{b_2})](V_{b_3})$$

We will use here a 100-mv LO signal into the differential pair and a 1000-mv AF signal at V_{b_3}. From the curves of figure 3.4, we have the following relation.

$$f_1(V_{b_3}) = (19.5 + 11e_{AF}\cos\omega_{AF}t)$$

This is a linear approximation to that curve which should provide sufficient accuracy for our purposes. Then, multiplying this by the LO voltage times R_L gives the following sum frequency. Other terms are not of interest here.

$$e_{o_1} = \text{other terms} + (11\frac{mv}{\text{volt peak}})(\frac{1\text{volt peak}}{1.41V\ RMS})(707mV)(\frac{1v}{1000mv})(100.)(\frac{1}{mv}x\frac{ma}{1000mv})$$
$$(\frac{1}{2})(100mv)$$

$$e_{o_1} = 25.3\ mv\ RMS$$

Now to deal with the second term we must apply Chaffee's method to the curve of figure 2.4, Mode D. Redrawing the curve delow in figure Ia, we strike off a circle at the differential bias point. Care must be

taken to insure that a residual offset is measured and recorded. The center of the circle must be placed at the measured value of offset even though the circuit is nominally zero biased at the differential input. Because of the rapidly changing g_m values away from zero bias, an offset as little as 3 or 4 millivolts will drastically affect the results.

The radius of the circle is that of the peak value of the sine wave considered. Then using a protractor to divide the cirlce into 30-degree sectors, we see from the illustration that we have marked off the 0, $\pm$ 0.5, $\pm$ 0.866, and $\pm$ 1.0 ratios of the normalized sine wave. (i.e. the ratio of the instantaneous value to the peak value). Because of space limitations, the illustration shows the sine wave rotated 90 degrees counter-clockwise from its actual position. The zero of the sine wave should actually be on the line of symmetry bisecting the g_m curve and passing through the center of the circle. Applying the formulae given earlier, we can now calculate the conversion transconductance of the first sum frequency.

$$g_{c_1} = \frac{1}{12}\left[(g_7 - g_1) + (g_5 - g_3) + 1.73(g_6 - g_2)\right]$$

$$= \frac{1}{12}\left[(0.8 - 0.8) + (7.2 - 8.3) + 1.73\ (1.3 - 2.0)\right]$$

$$= \frac{1}{12}\left[-1.1 - 1.21\right] = -\frac{1}{12}\ (2.31) = -0.19$$

We ignore the sign of this results since it is caused by the order in which the points on the g_m curve were labeled. Then calculating e_{o_2}, we have:

$$e_{o_2} = g_{c_1} R_L V_{b_3} = (0.19 m\mho)(100\Omega)(707 mv)(10^{-3}) = 13.4 mv$$

Summing the two components gives us: e_o = 25.3 + 13.4 = 38.7 millivolts. The measured value was 35 millivolts.

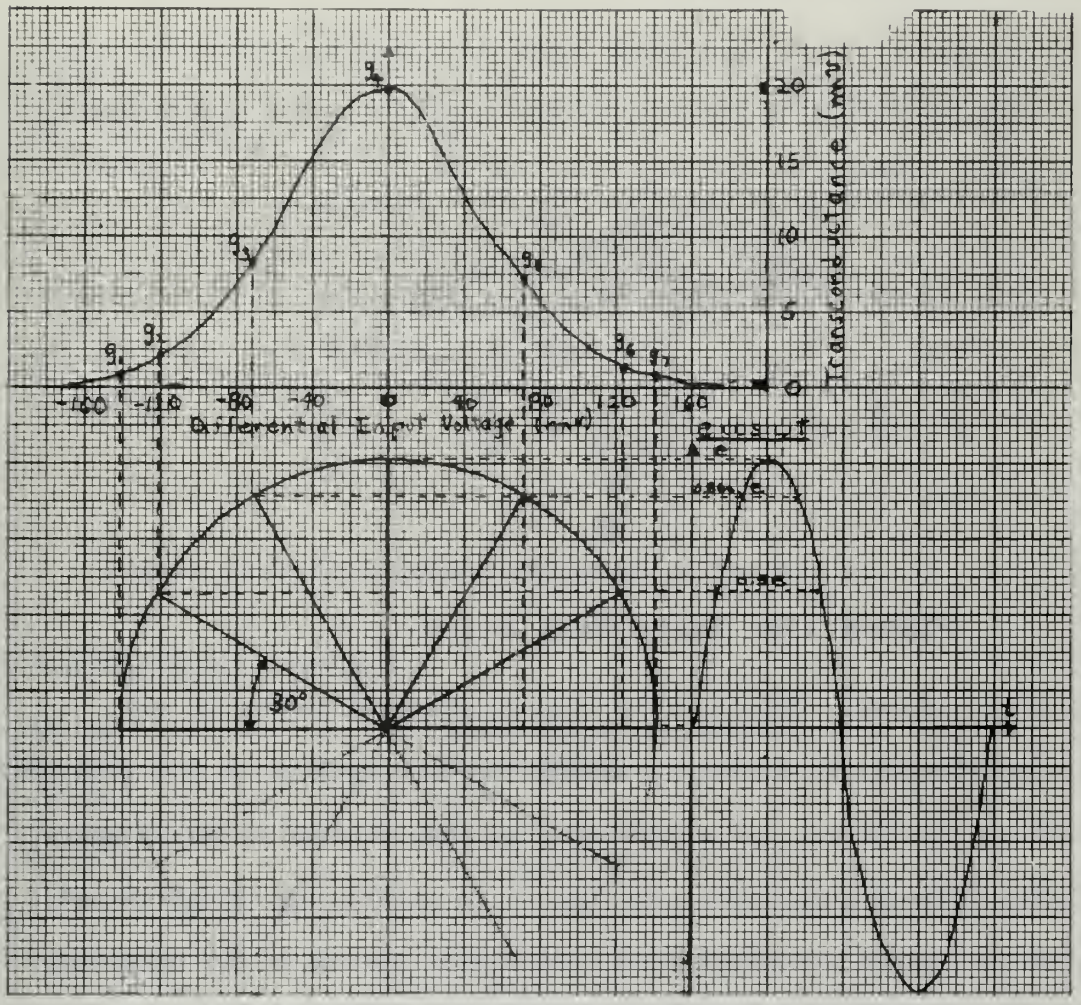

Figure Ia: Illustration of harmonic analysis of transconductance curve

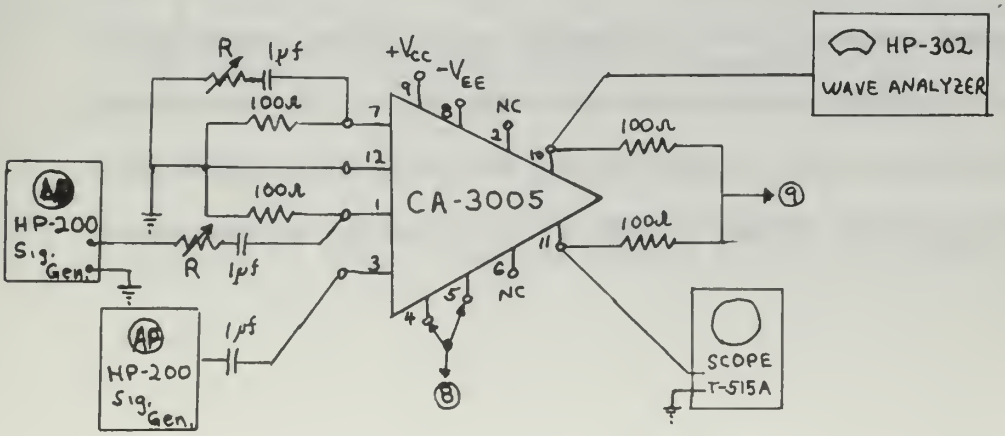

Appendix II

Suggested Laboratory Exercises

A schematic of the basic test board is shown in figure IIa. The 100 ohm resistors in the base leads at pins 7 and 1 were usually

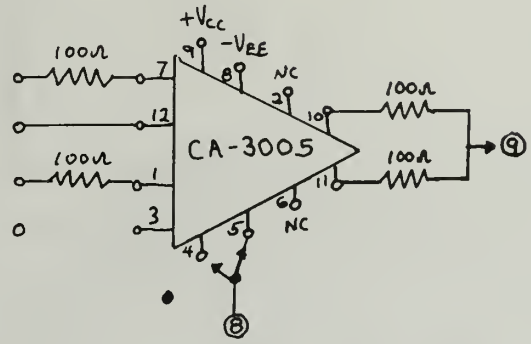

Figure IIa: Basic Test Board

returned to ground. Offset could then be measured and would not vary significantly as different equipments were applied to the terminals. The 100-ohm resistors also served as a voltage divider in cases where available voltage generators were unable to provide low-level signals. The 100-ohm output resistors were arbitrarily placed in the collector leads. This value was chosen to provide a convenient number for calculations and to provide as low a level of resistance as possible, to preclude swamping the device characteristics. A smaller value would create difficulties in obtaining output voltage readings for low-level harmonics. In order to maintain uniformity in developing device characteristics, supply voltage were adjusted to provide + 6 VDC at pins 10, 11 and - 6 VDC at pin 8 for all measurements.

No. 1 AF and LO signals injected into the differential pair

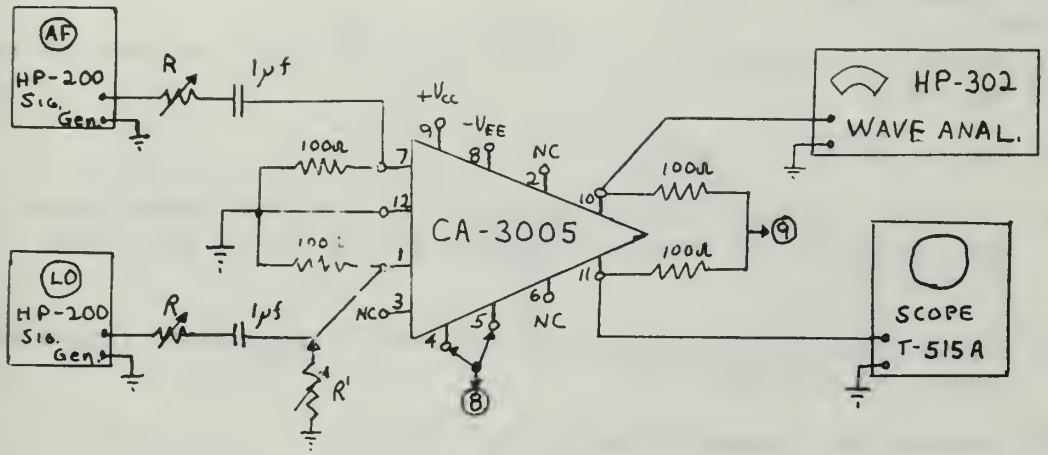

Figure II b: Test Board Configuration for No. 1

Test Equipment required:

HP-200	Audio Signal Generator	2 ea.
HP 721	Power Supply	2 ea.
HP 427	VTVM	1 ea.
Tectronix 515	DC Oscilloscope	1 ea.
GR-1432-J	10K Decade Resistor Box	3 ea.
1 uf capacitor		2 ea.

Procedure:

(1) Make all connections as shown in figure IIb except R'.

(2) Measure and adjust supply voltages so that pins 10, 11 read +6 VDC and pin 8 reads -6 VDC.

(3) With R set at about 1 K-ohm, adjust the AF signal generator for 5 mv measured at pin 7. Similarly set the LO signal generator at the first voltage level desired, measuring at pin 1. Both decade boxes, R, should have the same resistance values.

(4) Measure the D. C. Offset ($V_{B_1} - V_{B_7}$).

(5) Using the Wave Analyzer, record the frequency spectrum for each of several LO voltage settings through the third harmonic.

(6) Connect R' to provide D. C. Offset. Adjust R' to obtain an offset that places the Q point in the center of the linear portion of the g_m curve.

(7) Repeat steps 3 through 5.

(8) Adjust R' to provide D. C. offset near the cutoff segment of the g_m curve.

(9) Repeat steps 3 through 5.

(10) Calculate conversion gain and plot the calculated values with the LO voltage as the absissa using the first, second and third harmonics.

(11) Check results using the method outlined in Appendix I for selected values of each data run.

(12) Compare and discuss results.

No. 2 AF signal in the differential pair, LO signal in Q_3

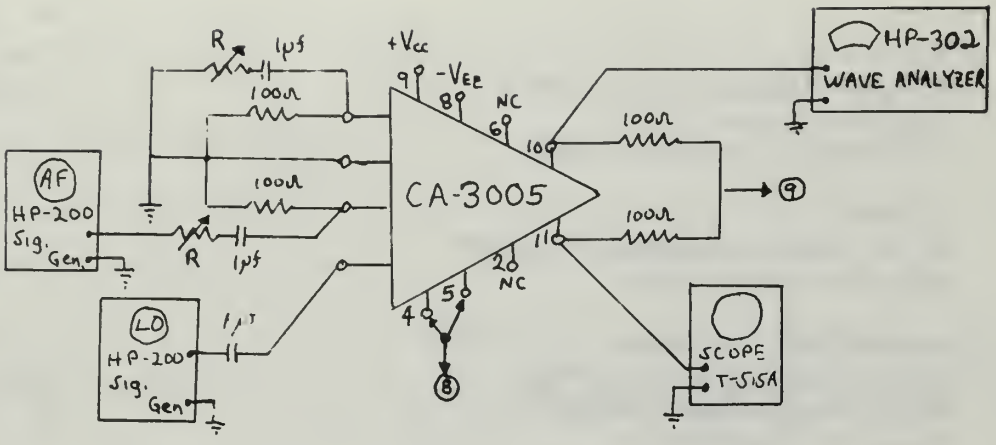

Figure IIc: Test Board Connections for No. 2

Test Equipment required is the same as that in No. 1

Procedure:

(1) Make all connections as shown in figure IIc except R'.

(2) Measure and adjust supply voltages so that pins 10, 11 read +6 VDC and pin 8 reads -6 DVC.

(3) With R set at about 1 K-ohm, adjust the AF signal generator for 5 mv. measured at pin 1. Set the LO generator at the first voltage level desired, measuring at pin 3. Both decade resistors, R, should be the same value.

(4) Measure the DC Offset ($V_{B_1} - V_{B_2}$).

(5) Using the Wave Analyzer, record the frequency spectrum for each of the several LO voltage settings through the third harmonic.

(6) Connect R' to provide D. C. Offset. Adjust R' to obtain an offset that places the Q point in the center of the linear portion of the g_m curve.

(7) Calculate conversion gain and plot the calculated values with the LO voltage as the absissa using the first, second and third harmonic.

(8) Check results using the method outlined in Appendix I for selected values of each data run. Be sure to locate the bias point at the value of offset measured between pins 1 and 7.

(9) Compare and discuss results.

INITIAL DISTRIBUTION LIST

		No. Copies
1.	Defense Documentation Center Cameron Station Alexandria, Virginia 22314	20
2.	Library U. S. Naval Postgraduate School Monterey, California	2
3.	Professor W. M. Bauer Electrical Engineering Dept. Naval Postgraduate School Monterey, California	1
4.	Commandant, USCG (PTP-2) Headquarters, U.S. Coast Guard Washington, D. C. 22214	1
5.	R. C. McFarland 3215 Ed Creighton Blvd. Omahaa, Nebraska 68105	1

DOCUMENT CONTROL DATA - R & D

Security classification of title, body of abstract and indexing annotation must be entered when the overall report is classified)

1 ORIGINATING ACTIVITY (Corporate author)
Naval Postgraduate School
Monterey, California 93940

2a. REPORT SECURITY CLASSIFICATION
Unclassified

2b. GROUP

3 REPORT TITLE
Investigation of a Monolithic, Integrated-Circuit, Differential Amplifier as a Mixing Device

4 DESCRIPTIVE NOTES (Type of report and, inclusive dates)
Thesis

5 AUTHOR(S) (First name, middle initial, last name)
McFarland, Robert Conrad

6. REPORT DATE
September, 1968

7a. TOTAL NO. OF PAGES
57

7b. NO. OF REFS

8a. CONTRACT OR GRANT NO.

b. PROJECT NO.

c.

d.

9a. ORIGINATOR'S REPORT NUMBER(S)

9b. OTHER REPORT NO(S) (Any other numbers that may be assigned this report)

10. DISTRIBUTION STATEMENT
[redacted] export controls and each transmittal to

11. SUPPLEMENTARY NOTES

12. SPONSORING MILITARY ACTIVITY
Naval Postgraduate School

13 ABSTRACT

The balanced, differential-amplifier configuration finds wide applicability in its monolithic integrated form. This paper investigates the use of the MIC differential amplifier as a mixer. The device chosen for this investigation permits signal injection both in the differentially driven pair and in the constant-current sink which biases the differential pair. Device characteristics pertinent to the mixing process are generated and discussed. On the basis of the experimentally derived characteristics, several different frequency conversion methods are employed and compared on the basis of conversion gain and distortion and intermodulation effects.

14 KEY WORDS	LINK A		LINK B		LINK C	
	ROLE	WT	ROLE	WT	ROLE	WT
Integrated circuit						
Differential Amplifier						
Mixer						